ELSEVIER

Ceramics International 33 (2007) 413–418

CERAMICS INTERNATIONAL

www.elsevier.com/locate/ceramint

Rare-earth substitution effect on the quality of Mg–Ti ferrite

M.M. El Sayed

Physics Department, Faculty of Education, Ain Shams University, Roxy, Cairo, Egypt

Received 14 July 2005; received in revised form 31 August 2005; accepted 23 September 2005
Available online 6 January 2006

Abstract

A series of ferrite samples of the chemical composition $Mg_{1+x}Ti_xR_yFe_{2-2x-y}O_4$; R = Ce and Er, $y = 0.025$ and $0 \leq x \leq 0.5$), in powdered form were prepared by standard double-sintering ceramic technique at 1200 °C using on-heating rate of 4 °C/min. X-ray diffraction analysis confirmed the single-phase spinel cubic structure for all samples. The dielectric constant (ε') and the ac electrical conductivity (σ) were studied at different temperatures as a function of the applied frequency. The Seebeck voltage coefficient was carried out for all samples to identify the type of charge carriers. The magnetic susceptibility was measured by the Faraday's method, where the sample was inserted at the maximum force point. By introducing a relatively small amount of R_2O_3 instead of Fe_2O_3, an important modification of structural, electrical and magnetic properties was achieved. The effect of rare-earth (RE) ions was explained by the partial diffusion in the spinel lattice.

Keywords: Mg–Ti ferrite-doped rare-earth dielectric; Magnetic susceptibility; Seebeck coefficient

1. Introduction

Ferrites have many applications in high-frequency devices, and they play a useful role in technological and magnetic applications because of their high electrical resistivity and sufficiently low dielectric losses over a wide range of frequencies [1].

Soft ferrites are being employed in wide range of applications and have contributed materially to advances in electronics [1]. In addition, they can be used as a channel filter in telephones, tone-generating circuitry of push button telephones and as load coils in transmission lines to reduce signal loss over long distances. Rare-earth (RE) ferrites have found an important application in modern telecommunications and electronic devices. Engineers and scientists [2] are interested to improve their preparation method and to determine their crystal structure dependence on composition as well as sintering conditions. RE ions can be divided into two categories [3]: the first one in which R ions with radius very close to the Fe ions can enter into the spinel lattice; while the second type with ionic radius larger than Fe ions. The electrical conductivity and dielectric behavior of spinel ferrites are very sensitive to the type of substituent and sintering conditions, such as temperature, time and heating rate. Study of the effect of these factors on the electrical properties offers much valuable information on the behavior of the localized electric charge carriers, which can lead to a good explanation and understanding of the mechanism of the electric conduction and the dielectric in ferrite behavior [4]. The addition of small proportions of RE ions to ferrite samples produces a change in their electrical as well as structural properties depending on the type and the amount of RE used. Several investigators have studied the frequency dependence of the dielectric properties of ferrites [5–8]. A remarkable peak was observed near T_c where the variation from the ferromagnetic phase to paramagnetic one takes place.

The electrical resistivity of $Mg_{1+x}Ti_xFe_{2-2x}O_4$ ferrite ($x = 0.1$, 0.2, 0.3, 0.4) at different temperatures was measured by Abbas et al. [9]. The resistivity of these ferrite is controlled by the cation concentration in the B-sites where the tetrahedral Fe^{3+} ions are mainly replaced by Mg^{2+} ions and the octahedral Fe^{3+} ions are replaced by Ti^{4+} ions. The electrical properties of ferrites were studied at different temperatures and frequencies by many other authors [10–17]. Purushan et al. [18] measured the Seebeck coefficient of the ferrite of the general formula $Mg_{1+x}Ti_xFe_{2-2x}O_4$ ($0.1 \leq x \leq 0.5$). They found that the sign of the Seebeck coefficient for all the samples is negative, indicating that the predominant conduction mechanism is due to hopping of electrons from Fe^{2+} to Fe^{3+} on the octahedral sites.

E-mail address: mmelsayed26@yahoo.com.

0272-8842/$32.00
doi:10.1016/j.ceramint.2005.09.025

The aim of the present work was to study the effect of preparation conditions as well as the replacement with small proportions of RE ions on the electric and magnetic properties of the investigated materials to improve their quality.

2. Experimental

Magnesium titanium ferrite doped with different RE ions (Ce and Er) was prepared using the double-sintering ceramic technique [17]. The prepared samples were of the general formula $Mg_{1+x}Ti_xR_yFe_{2-2x-y}O_4$, R = Ce and Er, $0.1 \leq x \leq 0.5$, $y = 0.025$. Analar grade oxides (BDH) were mixed in stoichiometric ratios using an agate mortar for 4 h for each sample. The mixture was transferred to an electric shaker and ball-milled for another 4 h. After that, the samples were pressed into pellets by uniaxial hydraulic pressing at 5×10^8 N/m^2. Pre-sintering was carried out at 900 °C for 10 h using Lenton furnace type UAF 16/5 (England) with heating rate of 4 °C/min, then cooled to room temperature with the same rate. The final sintering (firing) was performed at 1200 °C for 16 h with the same heating rate. For the electrical measurements, the two surfaces of each pellet were polished carefully to remove the surface layer from which the Mg^{2+} ions were evaporated during the sintering process. The two surfaces of each pellet were coated with silver paste (BDH) and checked for good conduction. The calcined ferrite powders were checked using X-ray diffractometer model (ProkerD8) with CuKα radiation of wavelength (λ = 1.5418 Å). The data of X-rays show that all samples exhibit spinel structure with the peak intensity depending on the concentration of magnetic ions in the lattices. The estimated amount of the crystalline secondary phases differs from one sample to another, although all specimens were prepared under identical conditions. This means that the formation of secondary phases in the ferrite during the sintering process is markedly affected by both type and amount of R_2O_3 used [19]. The real part of dielectric constant (ε') and ac electrical resistivity (ρ) were measured using a bridge (model 4275A multi-frequency LCR meter, Hewlett, Packard, USA) by the two-probe method [20] at different temperatures (300–800 K) as a function of the applied frequency in the range 10 kHz–2 MHz. The temperature of the sample was measured with an accuracy better than ±1 °C using a T-type thermocouple connected to the temperature controller where the junction of the thermocouple was in direct contact with the sample to prevent any temperature gradient.

3. Results and discussion

3.1. Electrical properties

3.1.1. Dielectric constant

Fig. 1 is a set of typical curves indicating the variation of the real part of the dielectric constant ε' with the absolute temperature for the ferrite $Mg_{1+x}Ti_xR_yFe_{2-2x-y}O_4$, $0.1 \leq x \leq 0.5$, $y = 0.025$, R = Ce and Er, as a function of the applied frequency ranging from 100 kHz to 4 MHz. The general trend

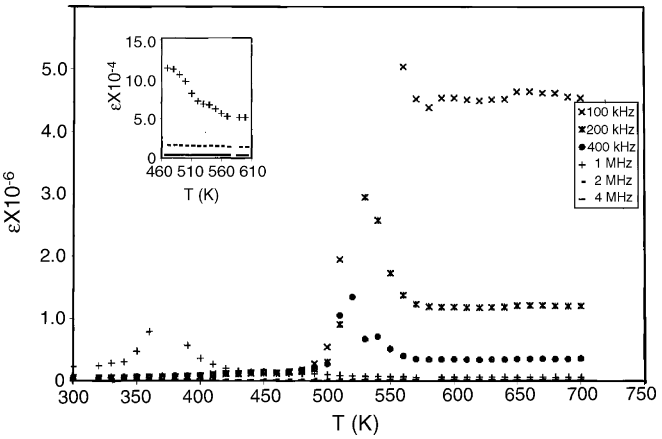

Fig. 1. Variation of the real part of the dielectric constant (ε') with absolute temperature at different electric field frequencies for the sample $Mg_{1+x}Ti_xR_yFe_{2-2x-y}O_4$, $x = 0.1$, R = Ce.

of the data is a slight increase in ε' (up to 500 K) followed by a large increase passing by the transition temperature for each sample. This may be due to the following: the small thermal energy given to the system is not sufficient enough to free more of the localized dipoles and the field oriented them in its direction. This means that ε' is nearly temperature-independent and the electronic polarization is the most predominant one. In the second region of temperature, ε' increases for all samples but with different rates depending on Ti concentration and the type of RE ions. This increase in ε' is due to electron hopping between the ferrous and ferric ions on the octahedral sites, which is maximum in case of minimum Ti concentration. Therefore, comparatively high ε' was obtained at $x = 0.1$ as shown in Fig. 1. This electron hopping causes a local displacement in the external field direction, producing change in polarization as well as ε' [15]. With increasing frequency, ε' decreases because the electric dipoles cannot follow-up the field variation. Also at high frequency, the alternation of the dipoles increases the friction between them leading to an increase in the quantity of heat generated. The energy dissipation is increased and the aligned dipoles will be disturbed with the result of decreasing ε'. Generally, for all investigated samples, ε' decreases with increasing frequency due to the field effect on the hopping process either between ions of the same element but with different valancies $Fe^{2+} \leftrightarrow Fe^{3+} + e^-$ or between different metal ions of different valancies, which means that the ac conductivity and dielectric are of the same origin. The data of ε' as a function of temperature for Ti content of 0.5 is shown in Fig. 2, different trend other than that of $x = 0.1$ is obtained except the effect of frequency. The value of ε' for $x = 0.1$ is much greater than for $x = 0.5$ (order of 10^3 times) which is the direct effect of both Ti ions substitution and the small additions of RE ions. This means that the addition of RE ions in the samples helps in forming aggregates on the grain boundary, which impedes the conduction process and increases the dielectric constant of the samples. This was enhanced by the data in Figs. 1–3. The results of the electrical resistivity agree well with this opinion.

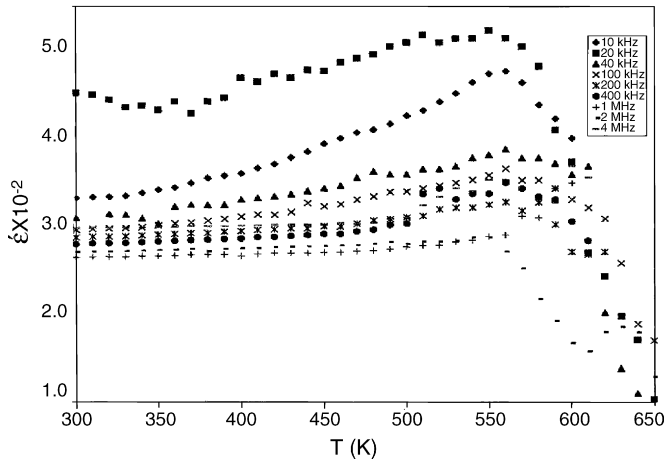

Fig. 2. Variation of the real part of the dielectric constant (ε') with absolute temperature at different electric field frequencies for the sample $Mg_{1+x}Ti_xR_yFe_{2-2x-y}O_4$, $x = 0.5$, R = Ce.

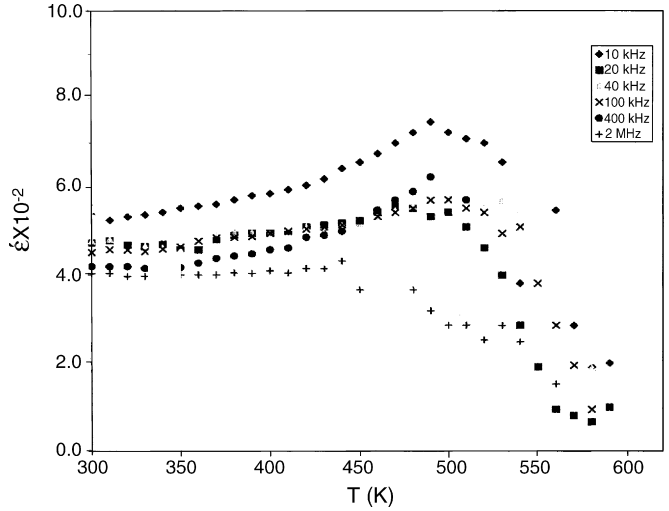

Fig. 3. Variation of the real part of the dielectric constant (ε') with absolute temperature at different electric field frequencies for the sample $Mg_{1+x}Ti_xR_yFe_{2-2x-y}O_4$, $x = 0.1$, R = Er.

3.1.2. Electrical conductivity

Fig. 4a and b is a typical curve correlating the ac conductivity ($\ln \sigma$) and the reciprocal of absolute temperature at different frequencies (10 kHz to 2 MHz) for the samples with $x = 0.1$, 0.5 and $y = 0.025$ in case of Ce-doped sample using heating rate 4 °C/min at sintering temperature 1200 °C. From the figure, it is clear that the data obeys the well-known Arrhenius relation [21], $\sigma = \sigma_o \exp(-E/kT)$, where σ_o is constant, k, E and T are the Boltzmanns constant, activation energy and the absolute temperature, respectively. Increasing temperature leads to an increase in σ, which is the normal behavior of semi-conducting ferrite. From a closer look to the data, one can find that more than one straight line were obtained with varying slopes indicating the existence of more than one conduction mechanism. In the paramagnetic region of disordered state, the increase in frequency has no effect on the conductivity corresponding to thermally activated charge carriers (band conduction mechanism) [22], while in the ferrimagnetic region the activation energy for electric conduction decreases as the frequency increases corresponding to the thermally activated mobility (hopping conduction model) [23] and not to thermally activated creation of charge carriers. As it was mentioned before the valance exchange, $Fe^{2+} \leftrightarrow Fe^{3+} + e^-$ is the main source of electron hopping in this process. The values of the activation energy as calculated from the experimental data are reported in Table 1. The small values of the activation energy in the ferrimagnetic region indicate the metallic-like behavior of the ferrite .The increase in the activation energy in the second region above 400 K (E_2) indicates the semi-conducting trend, which is almost the general behavior of ferrite materials. By increasing the frequency, the conductivity increases as a result of the pumping force of the applied frequency that helps in transferring the charge carriers between the different localized states as well as liberating the trapped charges from the different trapping centers. These charge carriers participate in the conduction process simultaneously with electrons produced from the valence exchange between the different metal ions. This mechanism continues up to a certain frequency after which the conductivity may decrease due to the disturbance effect of

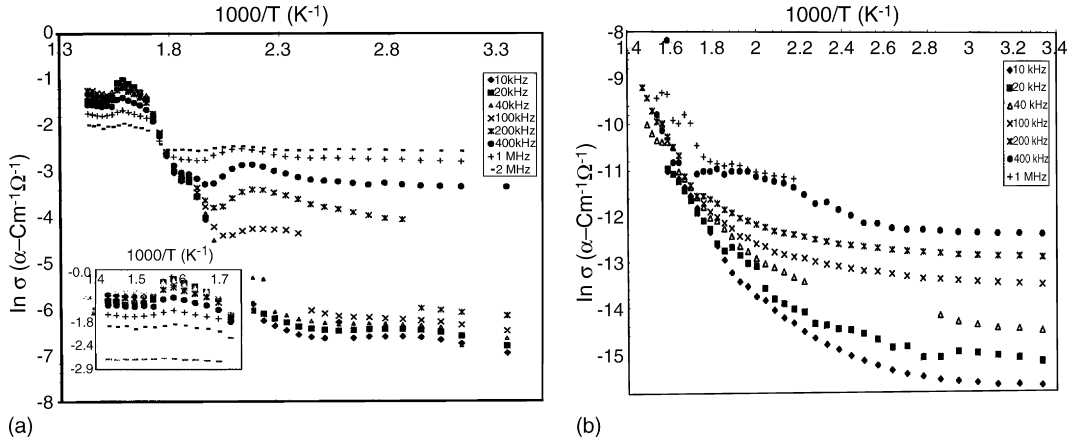

Fig. 4. Dependence of ln σ on the reciprocal of the absolute temperature at different electric field frequencies for the sample $Mg_{1+x}Ti_xR_yFe_{2-2x-y}O_4$: (a) Ce-doped sample, $x = 0.1$; (b) Ce-doped sample, $x = 0.5$.

Table 1
The activation energy in eV of $Mg_{1+x}Ti_x R_yFe_{2-2x-y}O_4$, for the low ($E_1$) and high ($E_2$) temperatures ranges at different Ti concentrations ($x = 0.1, 0.5$) and sintering temperature of 1200 °C and rate 4 °C/min

Frequency	R = Ce				R = Er	
	$x = 0.1$		$x = 0.5$			$x = 0.1$
	300–450 K[a] E_1(eV)	600–700 K[a] E_2(eV)	300–400 K[a] E_1(eV)	450–650 K[a] E_2(eV)	300–400 K[a] E_1(eV)	450–600 K[a] E_2(eV)
10 kHz	0.079	0.103	0.143	0.682	0.159	0.669
20 kHz	0.068	0.069	0.108	0.597	0.111	0.559
40 kHz	0.068	0.126	0.081	0.544	0.079	0.509
100 kHz	0.059	0.146	0.054	0.509	0.062	0.431
200 kHz	0.053	0.092	0.046	0.470	0.037	0.367
400 kHz	0.027	0.046	0.036	0.419	0.028	0.235
1 MHz	0.024	0.034	0.040	0.378	–	–
2 MHz	0.016	0.012	–	–	–	–

[a] T (K).

frequency. The change in the slope takes place around 400 K where the large value of the activation energy in the paramagnetic region is due to electron lattice phonons scattering. The small values of the activation energy in the low-temperature region confirm the electronic character of the conduction process, which consists of electron hopping between the ions of different valences. By increasing the temperature, the conductivity increases because the thermal energy helps in the conduction processes until reaching the peak value after which it decreases as the thermal energy becomes too large and so the polarization ceases. When increasing the Ti content, the activation energy increases. This was attributed to the masking effect of Ti^{4+} ions, which impedes the conduction.

The variation of the electrical resistivity at room temperature and the activation energy in the ferrimagnetic region is

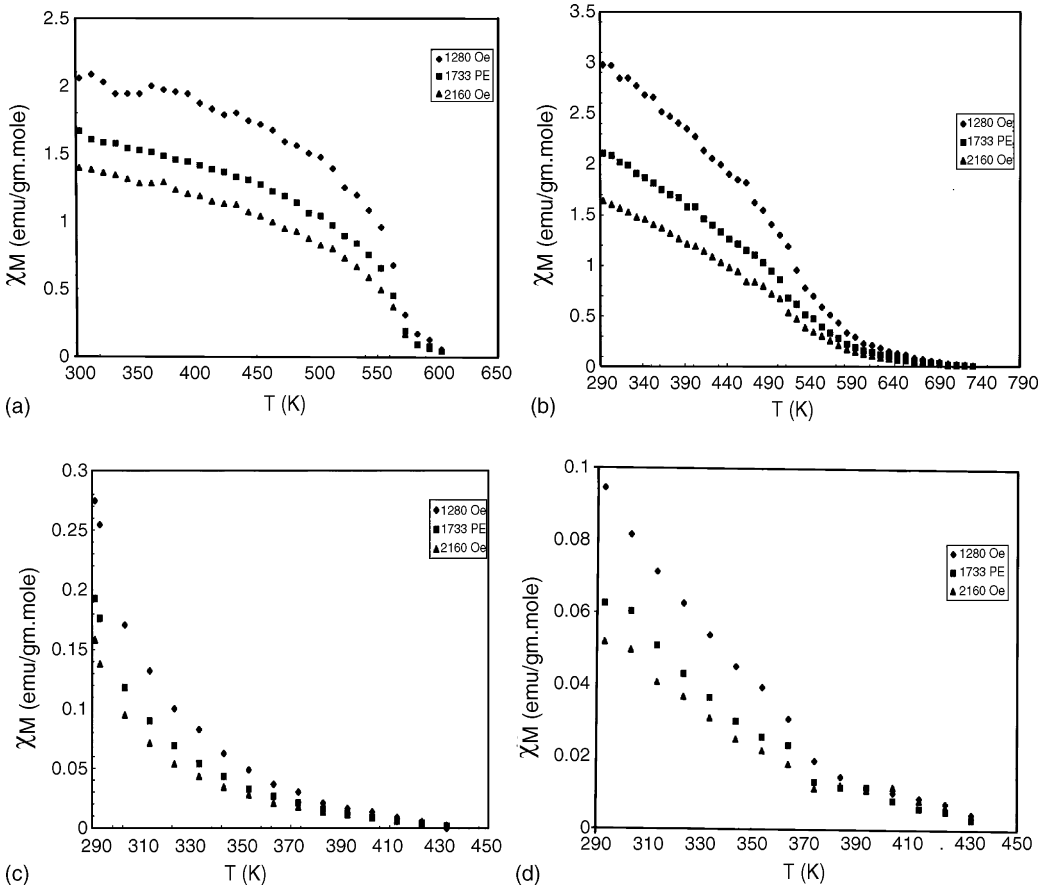

Fig. 5. Variation of the molar magnetic susceptibility (χ_M) with absolute temperature at different magnetic field intensities for the sample $Mg_{1+x}Ti_xR_yFe_{2-2x-y}O_4$: (a) Ce-doped sample, $x = 0.1$; (b) Ce-doped sample, $x = 0.5$; (c) Er-doped sample, $x = 0.1$; and (d) Er-doped sample, $x = 0.5$.

attributed to the ionic radius of the ions. This behavior could be explained by assuming that substituted RE ions enter into the B-site of the spinel structure where a single-phase cubic structure is obtained. The presence of RE ion at the B-site will increase the separation between Fe^{2+} and Fe^{3+} in proportion to its ionic radius. Thus, it impedes the electron transfer between Fe^{2+} and Fe^{3+}, i.e. it increases the activation energy and hence, the electrical resistivity according to its ionic radius.

3.2. Magnetic properties

It is known that [3] the magnetic properties of ferromagnetic oxides are governed by the Fe–Fe interaction (spin coupling of the 3d electrons). By introducing a small amount of RE ions (R) into the spinel lattice, the R–Fe interactions appear in a form of 3d–4f coupling leading to change in the magnetic behavior in the ferrite sample. Generally, an evaluation of this interaction can be obtained by analyzing the Curie temperature or magnetization. Fig. 5a–d is a typical curve showing the variation of the molar magnetic susceptibility (χ_M) with absolute temperature as a function of the magnetic field intensity (1280, 1733 and 2160 Oe) for the samples $Mg_{1+x}Ti_xR_yFe_{2-2x-y}O_4$, $0.1 \leq x \leq 0.5$, $y = .025$, R = Ce and Er. From the figure it is clear that the ferrimagnetic behavior can be observed for all samples, which are almost independent of the type of R ion. The data show that (χ_M) steadily decreased with increasing temperature before it dropped to very small value. One can divide the variation into two different regions: the first one is considered as a pure ferromagnetic region in which the thermal energy was not quite sufficient to disturb the aligned moments of the spins. In the last region of the temperature, the heat content of the system is too large so it can disturb all the aligned moments giving rise to complete paramagnetism. These observations are significant for various states [24]. It means that the value of magnetization decreases with increasing magnetic field intensity because of the replacement of some Ti^{4+} with Fe^{3+} ions on tetrahedral sites. Accordingly, the magnetic moments of the few remaining Fe^{3+} ions on the A sites are no longer able to be aligned anti-parallel with all the moments of the B ions. From the comparison between Fig. 5a–d, one can find that the stable region of (χ_M) and its value decreases due to the increase in the replacement of Fe^{3+} by Ti^{4+} ions. Another observation from the comparison was observed as a shift of T_c to lower value with the increase of Ti content. The observed variation in the Curie temperature may be explained on the basis of the exchange interactions. Besides, the increase of T_c for Er ion-substituted specimens than those of Ce ion indicates that in these materials the negative Fe–Fe interaction is the strongest one, and R–Fe interaction (4f–3d coupling) has a minor influence at high temperature [25–29]. The values of the magnetic constants are calculated from the experimental data of reciprocal of susceptibility and absolute temperature and reported in Table 2. From the reported data it is clear that, $\mu_{eff.}$ decreases with increasing both magnetic field intensity and Ti content, which is an acceptable behavior due to saturation of the moments by increasing the magnetic field intensity. Also since the Ti^{+4} ion is diamagnetic, therefore its existence decreases the magnetic interaction, which appears in a form of decreasing $\mu_{eff.}$ The small concentration of Ce or Er (0.025) gives the chance to these ions to enter the spinel lattice and replace some of the Fe^{3+} ions on the octahedral (B) site. This will change the ratio of Fe^{2+}/Fe^{3+}, which directly affects the conductivity and magnetic susceptibility. The effective magnetic moment of Ce^{3+} and Er^{3+} ions are 2.6 and 9.55 BM, respectively. The replacement of these ions in the investigated samples will drastically affect their magnetic properties, which is reflected in the values of χ_M of Er, which are 15 times larger than that of Ce (χ_M for Ce = 0.2, χ_M for Er = 3.0). The experimental values as calculated from the reciprocal molar susceptibility and reported in Table 2 enhance our expectation. The larger ratio of RE element does not enter the spinel lattice but form aggregates on the grain boundary forming a secondary phase, affecting directly the lattice parameter as well as the grain size. This work will be published later. The values of exchange interaction (J) can be calculated using the formula $J = \sqrt{3k_BT_C/2Z} \times S(S+1)$ where $Z = 8$; $S = 1/2$ and $k_B = 1.38 \times 10^{-17}$, and the values of molecular field constant (λ) calculated as $\lambda = T_C/C$ where C is the Curie constant. It is clear that the increases of Ti content decrease the value of exchange interaction and increase the values of molecular field constant.

Table 2
Values of magnetic constant as a function of the magnetic field intensity as calculated from the magnetic susceptibility data, the Curie constant (C), Curie temperature (T_c), effective magnetic moment ($\mu_{eff.}$), the exchange interaction constant (J) and molecular field constant (λ) for $Mg_{1+x}Ti_xR_yFe_{2-2x-y}O_4$; $0.1 \leq x \leq 0.5$; $y = 0.025$ and R = Ce and Er

Sample	Magnetic constant	1280 Oe	1733 Oe	2160 Oe
R = Ce, $x = 0.1$	C (emu/gm mole) K	0.40	0.32	0.23
	T_c (K)	605	605	605
	$\mu_{eff.}$ (BM)	1.80	1.59	1.35
	J (eV K)	4.57×10^{-8}	4.57×10^{-8}	4.57×10^{-8}
	λ	1512	1890	2630
R = Ce, $x = 0.5$	C (emu/gm mole) K	0.12	0.096	0.079
	T_c (K)	434	434	434
	$\mu_{eff.}$ (BM)	1.00	0.88	0.80
	J (eV K)	3.87×10^{-8}	3.87×10^{-8}	3.87×10^{-8}
	λ	3616	4520	5493
R = Er, $x = 0.1$	C (emu/gm mole) K	0.85	0.55	0.30
	T_c (K)	730	730	730
	$\mu_{eff.}$ (BM)	2.61	2.10	1.72
	J (eV K)	5.02×10^{-8}	5.02×10^{-8}	5.02×10^{-8}
	λ	858	1327	2433
R = Er, $x = 0.5$	C (emu/gm mole) K	0.11	0.07	0.05
	T_c (K)	432	432	432
	$\mu_{eff.}$ (BM)	0.93	0.76	0.62
	J (eV K)	3.86×10^{-8}	3.86×10^{-8}	3.86×10^{-8}
	λ	3927	6171	8640

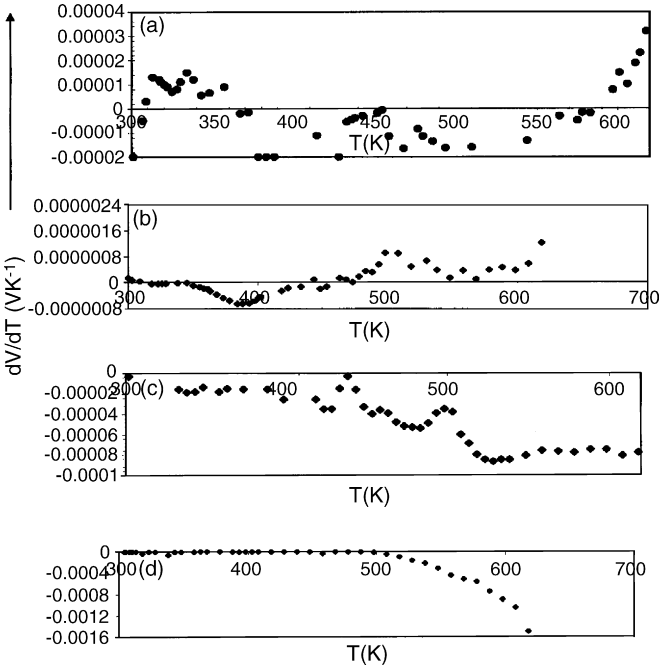

Fig. 6. Relation between Seebeck voltage coefficient (S) and average absolute temperature for the sample $Mg_{1+x}Ti_xR_yFe_{2-2x-y}O_4$: (a) Ce-doped sample, $x = 0.1$; (b) Ce-doped sample, $x = 0.5$; (c) Er-doped sample, $x = 0.1$; and (d) Er-doped sample, $x = 0.5$.

3.3. Thermoelectric power

Fig. 6a–d correlates the Seebeck voltage coefficient and average absolute temperature for the investigated samples. It is clear that the variation in the charge carriers between n- or p-type depends on R^{3+} type and size. The negative and positive values of thermoelectric power found over the entire temperature range Ce^{3+}-doped samples give positive Seebeck coefficient due to small positive polorons that participate in the conduction process, while Er^{3+}-doped samples give negative Seebeck coefficient. The above ferrites have been classified as n-type semi-conductors. Thus, the conduction mechanism for n-type is predominantly due to electrons that comes from changing Fe^{2+} to Fe^{3+} through the process $Fe^{2+} \leftrightarrow F^{3+} + e^-$.

The presence of thermoelectric power of more than one peak or region indicates the existence of more than one conduction mechanism, which was enhanced by the presence of more than one straight line in $\ln \sigma$ versus $1/T$.

4. Conclusion

(1) All investigated samples exhibit spinel structure whose peak intensity depends on the concentration of magnetic ions in the lattice.
(2) The values of ε' for $x = 0.1$ are much greater than those of $x = 0.5$ (order of 10^3 times), which is the direct effect of both Ti ions substitution and the small additions of RE ions.
(3) Increasing Ti content increases the activation energy as the result of the masking effect of Ti^{4+} ions, which impedes the conduction process.
(4) The variation of the electrical resistivity in the ferrimagnetic region is attributed to the ionic radius of the substituted ions.
(5) The replacement of some Ti^{4+} with Fe^{3+} ions on the tetrahedral site decreases the magnetization.
(6) The value of T_c was shifted to lower temperature with the increase of Ti content. The Er substitution increases the Curie temperature more than the Ce-substituted one.
(7) The value of χ_M of Er is15 times larger than for Ce (χ_m for Ce = 0.2, χ_M for Er = 3.0).

References

[1] A. Goldman, Modern Ferrite Technology, Marcel Dekker, New York, 1993.
[2] M. Ristic, S. Popovic, S. Music, J. Matter Sci. Lett. 9 (1990) 872–875.
[3] N. Rezlescu, E. Rezlescu, C. Pasnicu, M.L. Craus, J. Phys., Condens. Matter 6 (1994) 5707–5716.
[4] M.A. Ahmed, E. Ateia, G. Abdelatif, F.M. Salem, Mater. Chem. Phys. 81 (2003) 63–77.
[5] G.G. Koop's, Phys. Rev. 83 (1951) 121.
[6] G. Moltgen, Z. Angew Phys. 4 (1952) 216.
[7] L.G. Vanuitert, Proc. IRE 44 (1956) 1294.
[8] M.A. Ahmed, K.A. Darwish, E.H. El Khawas, J. Mater. Sci. 16 (1997) 1948.
[9] Y. Abbas, M.A. Ahmed, M.A. Semary, J. Mater. Sci. 18 (1983) 2890.
[10] M.A. El Hiti, J. Magn. Magn. Mater. 164 (1996) 187–196.
[11] K. Iwauchi, Y. Ikeda, Phys. Status Solidi A 139 (1992) 499.
[12] K. Iwauchi, M. Kiyama, T. Nakamara, Phys. Status Solidi A 127 (1991) 499.
[13] C. Prakash, J.S. Baijal, J. Less-Common Met. 107 (1985) 51–57.
[14] J.C. Maxwell, Electricity and Magnetism, Oxford University Press, London, 1973, p. 328.
[15] P.V. Reddy, T.S. Reo, J. Less-Common Met. 86 (1982) 255–261.
[16] M.A. Ahmed, E.H. El Khawas, F.A. Radwan, J. Matter. Sci. 36 (2001) 5035.
[17] M.A. Ahmed, S.T. Bishay, G. Abdelatif, J. Phys. Chem. Solids 62 (2001) 1039.
[18] Y. Purushan, V.R. Reddy, D.R. Sigar, P. Kishan, P. Reddy, Phys. Status Solidi A 140 (1993) K29.
[19] E. Rezlescu, N. Rezlescu, P.D. Popa, L. Rezlescu, C. Pasnicu, Phys. Status Solidi A 162 (1997) 673.
[20] K. Vijaya Kumar, D. Ravinder, Matter Lett. 52 (2002) 166.
[21] J. Smit, H.P. Wijn, Ferrite, Cleaver Hume Press, London, 1959.
[22] M.A. Ahmed, M.A. El Hiti, Magn. Mater. 146 (1995) 84.
[23] M.A. Ahmed, S.T. Bishay, J. Phys. D Appl. Phys. 34 (2001) 1–7.
[24] S. Unnikrishanan, D.K. Chakrabaty, Phys. Status Solidi A 121 (1990) 265.
[25] L.A. Vladimirtseva, G.V. Samsonov, V.A. Gorbatyuk, Powder Metall. Met. Ceram. 12 (8) (1973) 669.
[26] R. Krishan, V. Cagan, IEEE Trans. Magn. MAG-79 (1971) 613.
[27] L.G. Vanuitert, J. Appl. Phys. 26 (1955) 1289.
[28] M. Singh, S.P. Sud, Mater. Sci. Eng. B: Solid State Mater. Adv. Technol. 83 (1–3) (2001) 180.
[29] A.K. Rastogi, G. Hilscher, E. Gratz, N. Pilmay, J. Phys. 49 (1988) 277.